Numerical Simulations of a Low-Power Cylindrical Hall Thruster Under Development at the University of Brasilia

Gabriele Almeida dos Santos[1], Rodrigo A. Miranda[1, 2], Sérgio Thadeu Tavares da Silva Júnior[1], and José L. Ferreira[2]

[1]*Faculty of Science and Technology in Engineering, University of Brasilia, Brasilia-DF, Brazil.* [2]*Laboratory of Plasma Physics, Institute of Physics, University of Brasilia, Brasilia-DF, Brazil.* ,
**corresponding author:gaby.almeida99@gmail.com*

Received: Outubro/2025; Accepted: Novembro/2025; Published: Novembro/2025

Abstract: The cylindrical Hall thruster (CHT) is an electric propulsion system proposed for nanosatellites (e.g., CubeSats) due to its efficiency, structural simplicity and compact size. Unlike conventional Hall thrusters with annular geometry, the CHT has a cylindrical configuration that can reduce wall erosion and facilitate miniaturization. We perform numerical simulations of a CHT operating at low power, focusing on voltage ranges between 50 V and 150 V at the anode. This operating range is particularly important for small satellites, which are subject to strict power consumption limitations. The methodology applied in this work involves the use of two open source software tools: Finite Element Method Magnetics (FEMM), which is used to model the magnetic field of the thruster, and the Hall Ion Source Simulator (HALLIS), which simulates the behavior of the plasma using a hybrid model, which means that electrons are treated as a fluid, while ions and neutral atoms are modeled as individual particles.

Keywords: Cylindrical Hall, Numerical Simulation, Low Power, Thruster.

1 Introduction

With the growing adoption of CubeSats and other nanosatellites in space missions, there is an increasing need for propulsion systems that combine compact size, low power consumption, and reliable performance. One technology that aligns well with these demands is the *Cylindrical Hall Thruster (CHT)* — a variation of the conventional Hall effect thruster that replaces the traditional annular discharge chamber with a cylindrical one. This change in geometry not only simplifies the thruster's structure but also helps reduce wall erosion, a common issue in long-duration operations, making it highly suitable for miniaturized spacecraft.

The CHT operates by creating a radial magnetic field that confines electrons within a cylindrical channel. A propellant gas is introduced through a centrally placed anode, and the trapped electrons ionize the neutral atoms through collisions. The resulting ions are then accelerated by an electric field established between the anode and an external cathode, producing thrust. This configuration allows efficient plasma generation and ion acceleration, even under limited power availability — a critical factor for small satellite platforms.

In this work, we conduct numerical simulations to investigate the performance of a low-power CHT within an operating voltage range of 50 V to 150 V. These values are selected to reflect the power constraints typically encountered in nanosatellite missions. Two open-source computational tools are

employed: *Finite Element Method Magnetics (FEMM)* is used for magnetic field design and analysis, while *HALLIS (Hall Ion Source Simulator)* is used to simulate the plasma behavior. The latter adopts a hybrid modeling approach, treating electrons as a fluid and handling ions and neutrals as discrete particles.

The insights gained from these simulations will support the development of a functional prototype at the University of Brasília. By evaluating plasma density profiles, magnetic field configurations, and performance metrics, this study contributes to the advancement of low-cost, high-efficiency electric propulsion solutions tailored to the needs of small-scale space exploration. This paper is organized as follows. Section 2 presents the software employed for the numerical simulations. Section 3 describes the CHT in detail. Section 4 contains the results from the numerical simulations, including the spatial profiles of the electric potential, the plasma density, and the operational parameters estimated from the simulations. Finally, our conclusions are given in Section 5.

2 Methodology

To carry out the simulation, two specialized software tools were used, each with a specific role in the process. The first is Finite Element Method Magnetic (FEMM), which was employed for generating the geometric model and for analyzing the electromagnetic field associated with the system. This software is widely used in studies involving the finite element method to solve electromagnetic problems with high precision.

The second software used was HALL Ion Sources (HALLIS), responsible for simulating the generation and behavior of the plasma within the system. HALLIS enables detailed plasma modeling, providing essential data on parameters such as plasma power and density under specific conditions—particularly at low power levels, where the behavior may exhibit unique characteristics.

The combination of these two software tools enables an integrated and accurate analysis of the phenomena involved, allowing for the validation and correlation of the results obtained, especially with regard to the power and density of the generated plasma, which are fundamental to the efficiency and performance of the system under study.

2.1 Finite Element Method Magnetic

For the simulations performed using the FEMM (Finite Element Method Magnetic) software, the magnetic field lines are generated based on Maxwell's equations, considering the magnetic field as a low-frequency problem. As a result, displacement currents are neglected (1). The simulations are based on the following equation

$$\nabla \times \frac{\nabla \times \mathbf{A}}{\mu(B)} = \sigma(\dot{\mathbf{A}} - \nabla V) \tag{1}$$

where $\mu(B)$ is the magnetic permeability, which may be a nonlinear function of the magnetic flux density B; σ is the electrical conductivity of the material; $\dot{\mathbf{A}}$ is the time derivative of the magnetic vector potential; and V is the electric scalar potential. Equation (1) leads to a partial differential equation representing the behavior of the magnetic field:

This formulation results from combining Maxwell's equations under the quasi-static (low-frequency) assumption, in which displacement currents are neglected. It is particularly useful for simulating electromagnetic fields in conductive regions using finite element methods, as implemented in FEMM.

2.2 HALL Ion Sources

The Hallis software is a plasma simulation tool that uses a hybrid model: electrons are treated as a fluid, while ions and neutral atoms are represented by pseudoparticles. Simulations can be performed in 1D or 2D. In this work, the 2D configuration was used. The fluid model for electrons considers

the continuity, momentum, and energy equations (with Maxwellian velocity distribution). Electron and atom collisions with the thruster walls are also taken into account. In the 2D model, equilibrium between the electric force and the pressure gradient along magnetic field lines is assumed, that is, the Morozov approximation is adopted.

2.2.1 Electron Mobility

Electrons in the software move parallel and perpendicular to the magnetic field. The model will only produce results consistent with experiments if the collision frequency is sufficiently high. These high collision frequencies are associated with electron collisions with the walls or turbulence effects.

$$\mu_{\parallel} = \frac{e}{m} \cdot \frac{\Omega_{ce}}{\nu^2 + \Omega_{ce}^2} \quad \text{and} \quad \mu_{\perp} = \frac{e}{m} \cdot \frac{\nu}{\nu^2 + \Omega_{ce}^2} \tag{2}$$

where $\mu_{\parallel}$ is the electron mobility parallel to the magnetic field (in $m^2/V{\cdot}s$); $\mu_{\perp}$ is the electron mobility perpendicular to the magnetic field; e is the electron charge ($\approx 1.602 \times 10^{-19}$ C); m is the electron mass ($\approx 9.109 \times 10^{-31}$ kg); ν is the electron collision frequency (with neutral particles, ions, or walls); and Ω_{ce} is the electron cyclotron frequency.

2.2.2 Ion Transport

Ion trajectories are calculated using the equation of motion under the influence of the electric field:

$$m_i \frac{d\vec{v_i}}{dt} = q_i \vec{E} \tag{3}$$

where m_i is the ion mass; q_i is the ion charge; $\vec{v_i}$ is the ion velocity; and $\vec{E}$ is the electric field.

2.2.3 Electron Temperature

The plasma temperature can be determined from the density and the electric field. The electron temperature is obtained by integrating the energy equation, assuming a Maxwellian velocity distribution. The distribution is given by:

$$f(v) = \left(\frac{m}{2\pi k_B T_e}\right)^{3/2} \exp\left(-\frac{mv^2}{2k_B T_e}\right) \tag{4}$$

where f(v) is the probability distribution function; m is the electron mass; k_B is the Boltzmann constant; T_e is the electron temperature; and v is the velocity.

The electron energy equation is:

$$\frac{\partial}{\partial t}\left(\frac{3}{2} n_e k_B T_e\right) + \nabla \cdot \left(\frac{5}{2} n_e k_B T_e \vec{u_e}\right) = Q - R \tag{5}$$

where n_e is the electron density; T_e is the electron temperature; $\vec{u_e}$ is the average electron velocity; Q is the energy source term; and R is the energy loss term (such as due to collisions or radiation).

2.2.4 Electric Field

The electric field is calculated based on the current continuity equation, requiring information on plasma density, ion flux, electron temperature, and electron mobility. In the 2D model, electrons do not move isotropically, and thus the equations are treated as tensor equations.

$$\nabla \cdot (n\mu_e \mathbf{E}) = \nabla \cdot [\mathbf{\Gamma}_e - \mu_e \nabla(nT_e)] \quad (6)$$

where n is the particle density; μ_e is the electron mobility; $\mathbf{E}$ is the electric field vector; $\mathbf{\Gamma}_e$ is the electron flux; and T_e is the electron temperature.

2.2.5 Neutral Atom Transport

The simulation includes atom-wall collisions and ionization. Atoms are injected into the channel with a semi-Maxwellian distribution and can also be regenerated from recombination at the channel walls. The average velocity is calculated as:

$$\overline{v_x} = \int_0^\infty v_x \, g(v_x) \, dv_x \quad (7)$$

where $\overline{v_x}$ is the average axial velocity component; v_x is the velocity component; $g(v_x)$ is the velocity distribution function in the x-direction; and v_T is the thermal velocity (typically defined as $v_T = \sqrt{2kT/m}$).

3 Cylindrical Hall Thruster

Hall thrusters are a type of electric propulsion device and exhibit high exhaust velocities as well as high specific impulse (2). Although they have lower efficiency compared to ion thrusters, Hall thrusters produce higher thrust and require less electrical power to operate (3).

The Hall thruster operates with a radial magnetic field generated by coils or permanent magnets and contains an anode and a cathode. Due to the action of the magnets, ions are accelerated in the annular chamber, generating thrust. Meanwhile, electrons become trapped in the chamber, creating the Hall current (2).

This article presents a cylindrical Hall thruster simulated with permanent magnets, designed to operate at low power levels ranging from 50 to 300 W. These thrusters are lighter compared to those using electromagnetic coils, which can consume up to 100 W and reduce system efficiency. Furthermore, the external electromagnetic fields generated by permanent magnets are stronger, contributing to increased specific impulse (4).

Ionization occurs in the annular region of the thruster, where doubly charged ions are produced, resulting in thrust generation. In the model proposed in this article, the thruster does not feature an annular channel, which helps extend the device's operational life by avoiding electron collisions with the channel walls.(5)

The absence of the annular channel significantly reduces structural degradation, allowing for longer continuous operation during extended missions. Additionally, the use of permanent magnets simplifies the thermal design of the thruster, as it eliminates the need for active cooling of the coils. The cylindrical geometry favors magnetic confinement of the plasma, optimizing the efficiency of ion acceleration. This configuration has proven to be promising for applications in CubeSats and small observation satellites.

4 Results and Discussion

4.1 FEMM

The magnets used to generate the simulation in the FEMM software are made of samarium-cobalt 32. The simulations were performed using a 2D model with a symmetric shape to generate the electromagnetic field. Since it is a 2D image, the simulation was defined as a semicircle contained within a boundary condition consisting of 7 layers, preventing external influence.

The magnets have the following dimensions: the first one measures 10 x 10 cm, and the other two measure 2 x 10 cm each. The mesh, with 11,841 nodes, generated between the magnets and the chamber was created by the software itself, maintaining uniformity and high resolution for the electromagnetic field calculations. At the end of the simulation, the data generated in a FEMM file are used to start the simulation in the HALLIS software, which processes the data to generate the simulated density, power and plasma.

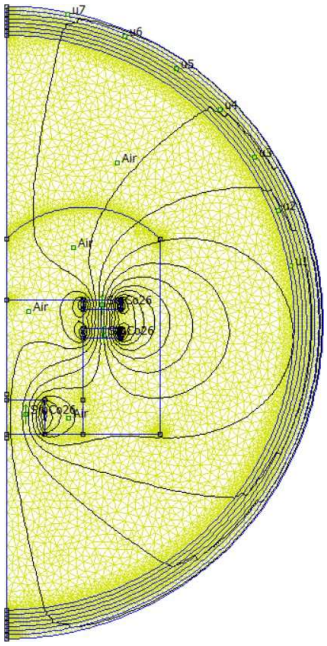

Figure 1.: Simulation domain in FEMM, showing the generated mesh nodes, the internal structure of the CHT, and magnetic field lines.

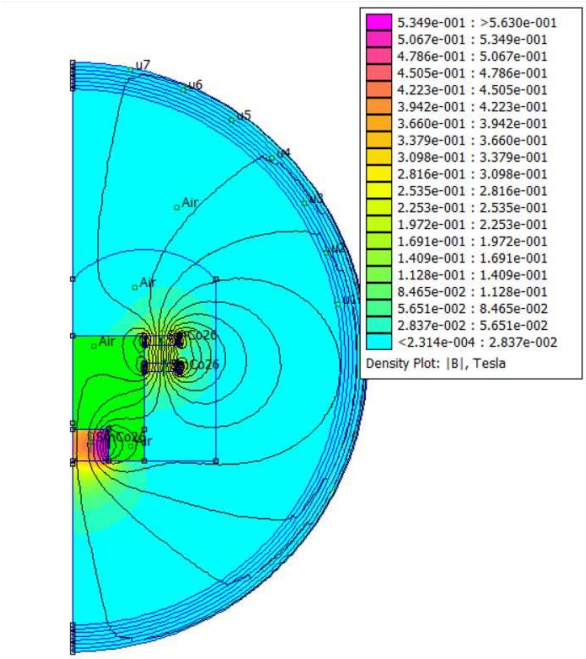

Figure 2.: Simulation domain in FEMM, showing the magnetic field intensity (color-coded), and the magnetic field lines.

4.2 HALLIS

Using the Hallis software, it is possible to simulate various configurations of the cylindrical Hall thruster, allowing for a detailed analysis of its performance under different operational conditions. In this study, voltage levels of 50 V and 150 V were considered for the simulations, aiming to evaluate the thruster's behavior under different electrical power inputs. Table 1 presents the main parameters adopted, as well as the boundary conditions applied to carry out the numerical experiments. Based on these parameters, results were obtained for the electrical power consumption and the plasma density generated inside the thruster, providing essential information for understanding the device's operation and guiding its optimization.

Table 1.: Simulation Parameters: Domain, Channel, and Component Positions

Section	Parameter	Value (cm)	Cells
Domain	Axial	5.000	50
	Radial	5.000	60
Channel	Length	2.500	25
	Inner radius	0.000	0
	Outer radius	2.000	40
Positions	Gas inlet (inner)	1.250	–
	Gas inlet (outer)	1.750	–

Next, we present the results for voltages ranging from 50 to 150 V. It is observed that the electrostatic potential reaches its maximum near the anode and gradually decreases along the axial direction toward the channel exit. Plasma density is highest near the central axis (Y = 0), with a localized peak close to the anode, caused by collisions between trapped electrons and neutral atoms, which enhance ionization. The plasma density distributions shown in Figures 6 and 7 also reveal a narrow region extending from the anode to the central area at the channel exit, where the highest values are recorded.

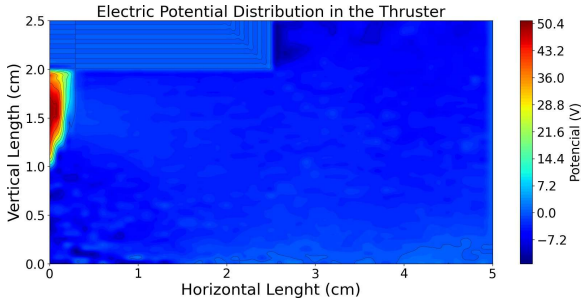

Figure 3.: Anode at 50 V

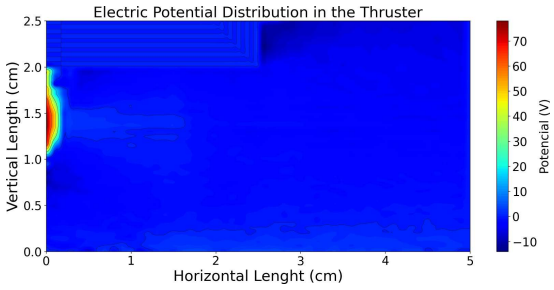

Figure 4.: Anode at 75 V

Figure 5.: Electric potential for low anode voltages (50 V and 75 V)

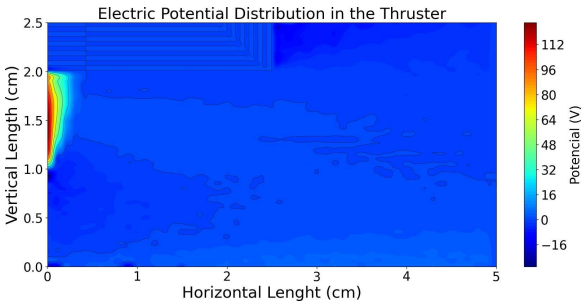

Figure 6.: Anode at 125 V

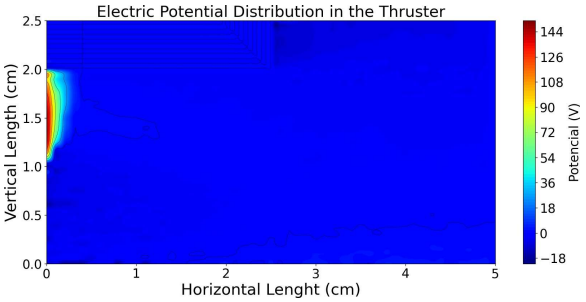

Figure 7.: Anode at 150 V

Figure 8.: Electric potential for high anode voltages (125 V and 15 V)

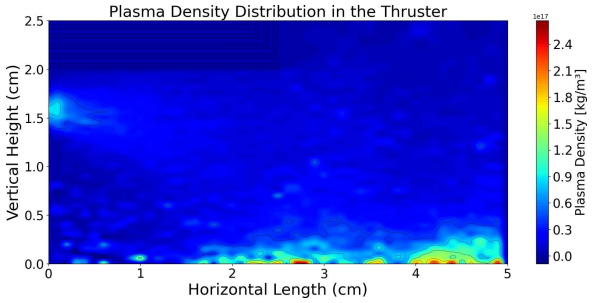

Figure 9.: Anode at 50 V

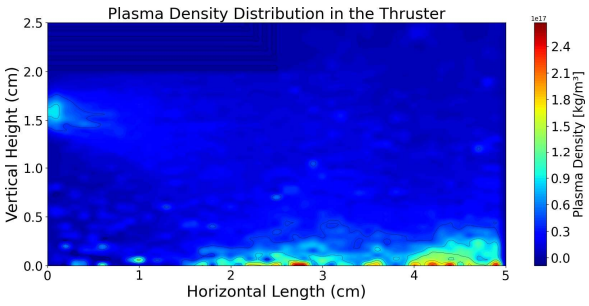

Figure 10.: Anode at 75 V

Figure 11.: Plasma density for low anode voltages (50 V and 75 V)

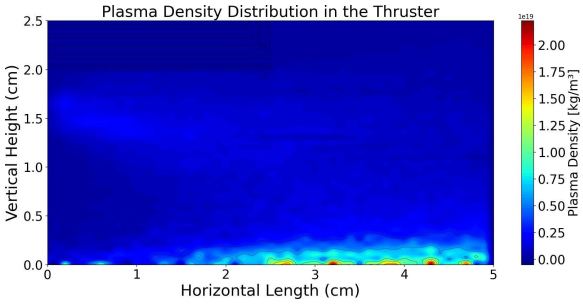

Figure 12.: Anode at 125 V

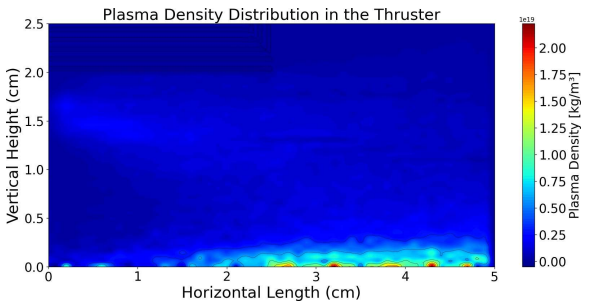

Figure 13.: Anode at 150 V

Figure 14.: Plasma density for high anode voltages (125 V and 150 V)

4.3 Performance Analysis

In this section we discuss the operational parameters computed from the numerical simulaions. The efficiency is related to the propulsion system performance and can be expressed as:

$$\eta_R = \frac{1}{2}\frac{T^2}{\dot{m}_a P} \tag{8}$$

where η_R is the thrust efficiency, T is the thrust, $\dot{m}_a$ is the anode mass flow rate, and P is the input power.

Specific thrust, or Specific Impulse (Isp), is the amount of thrust generated per unit mass flow rate of the propellant and is given by:

$$I_{sp} = \frac{T}{\dot{m} g_0} \tag{9}$$

where $\dot{m}$ is the mass flow rate of the propellant and g_0 is the standard gravitational acceleration.

The Specific Impulse based on ion velocity (Isp Ion velocity) is defined as the ratio of the average ion exhaust velocity V_{ion} to the gravitational acceleration:

$$I_{sp,ion} = \frac{V_{ion}}{g_0} \tag{10}$$

This expression represents how efficiently the propulsion system converts ion kinetic energy into useful thrust.

The operational parameters obtained from the numerical simulations are summarized in Table 2. From these results it is clear that all parameters increase with the available power, as expected.

Table 2.: Hall thruster performance at different voltages

Voltage (V)	Efficiency	Thrust (mN)	ISP (s)	ISP Ion velocity (s)	Power (W)
50	0.001	0.169	3.44	610.68	2.399
75	0.008	0.867	17.68	679.10	10.278
125	0.127	14.472	295.04	791.33	166.852
150	0.194	22.435	457.38	907.00	263.98

5 Conclusions

In this paper we presented results of numerical simulations of a CHT operating at low power, focusing on voltage ranges between 75 V and 150 V at the anode. This operating range is particularly important for small satellites, which are subject to strict power consumption limitations. The numerical simulations were performed using two numerical codes freely available on the internet, namely, the Finite Element Method Magnetics, which is used to model the magnetic field of the thruster, and the Hall Ion Source Simulator, which simulates the behavior of the plasma using a hybrid model. The numerical codes were discussed in detail.

The analysis of the electrostatic potential reveals a significant drop along the thruster channel, which is directly associated with the position of the anode, located at the center of the system. The plasma density images (Figure 5 and 6) show a pronounced accumulation in the annular region near the channel exit ($x < 1.5$ cm) and around the anode. Additionally, there is a formation of a high-density plasma band extending from the anode to the central region at the exit, indicating a greater concentration of particles in this area. This behavior is intensified with the increase of the voltage applied to the anode, promoting higher ionization. This occurs due to the presence of electrons trapped in regions of stronger magnetic fields, which collide with neutral atoms, increasing the plasma density.

In the simulation at 125 V, regions with plasma densities up to 2.25×10^{19} m^{-3} were identified, whereas at 150 V the maximum observed value was 1.35×10^{19} m^{-3}, highlighting the influence of the applied voltage on the plasma distribution. This behavior will be analyzed more thoroughly in future work to better understand the physical mechanisms responsible for this variation and its implications for thruster performance.

Although it performs lower compared to operation at 300 V, the thruster operating at 150 V shows very promising results, including higher efficiency compared to the 125 V simulation. Data indicate that efficiency increases from about 12.7% to 19.4% when moving from 125 V to 150 V, with a significant increase in thrust and specific impulse. This improvement suggests that operating at 150 V is an effective alternative to optimize performance while maintaining power consumption at levels suitable for CubeSat applications.

The use of permanent magnets to generate the magnetic field becomes a viable solution to reduce the thruster's power consumption, allowing it to operate in the range between 50 and 150 W. This feature is especially attractive for small space missions since it allows the saved energy to be redirected to other spacecraft subsystems. Thus, the design of a thruster operating at 150 V emerges as an effective option for assembly and testing in CubeSat missions. In addition to the values of the electric potential set in this paper, we are currently exploring higher values of the potential while keeping the total power constant. This will be the topic of a future work.

5.1 Declaration of Competing Interest

The authors declare that they have no competing interests.

5.2 Acknowledgements

GAdS acknowledges support from FAPDF, Brazil (grant 383/2023). RAM acknowledges support from CNPq, Brazil (grants 407341/2022-6, 407493/2022-0), FAPDF, Brazil (grant 383/2023) and the Brazilian Space Agency (TED 000529/2024). JLF acknowledges support from CNPq (grant 405907/2022-2) and the Brazilian Space Agency (TED 000529/2024). All numerical simulations were performed using computational resources at the Laboratory for Simulation of Plasma and Electric Propulsion (LaSPPE) at the Institute of Physics, UnB.

References

1 MEEKER, D. *Finite Element Method Magnetics*. 2025. <http://www.femm.info>. Accessed: 2025-07-14.

2 BRAGA, L. L.; MIRANDA, R. A. Particle-in-cell numerical simulation of the phall-iic hall thruster. *Plasma Physics Laboratory*, 2019.

3 GOEBEL, D. M.; KATZ, I. *Fundamentals of Eletric Propulsion: Ion and Hall Thruster*. [S.l.]: JPL SPACE SCIENCE AND TECHNOLOGY SERIES, 2008.

4 RAITSES, Y.; MERINO, E.; FISCH, N. J. Cylindrical hall thrusters with permanent magnets. *JOURNAL OF APPLIED PHYSICS*, 2010.

5 GARRIGUES, L.; HAGELAAR, G. J. M. Simulations of a miniaturized cylindrical hall thruster. *IEEE TRANSACTIONS ON PLASMA SCIENCE*, 2008.